IEEE Open Journal of Nanotechnology

Received 14 November 2021; revised 11 December 2021; accepted 12 December 2021. Date of publication 15 December 2021; date of current version 21 January 2022. The review of this article was arranged by Associate Editor Lianqing Liu.

Digital Object Identifier 10.1109/OJNANO.2021.3135478

Carbon-Based THz Microstrip Antenna Design: A Review

GUANXUAN LU, JIAQI WANG, ZHEMIAO XIE, AND JOHN T. W. YEOW (Senior Member, IEEE)

Department of Systems Design Engineering, University of Waterloo, Waterloo, ON N2L 3G1, Canada

CORRESPONDING AUTHOR: JOHN T. W. YEOW (e-mail: jyeow@uwaterloo.ca)

This work was supported in part by Natural Sciences and Engineering Research Council Canada (NSERC). *(Guanxuan Lu and Jiaqi Wang contributed equally to this work.)*

This article has supplementary downloadable material available at https://doi.org/10.1109/OJNANO.2021.3135478, provided by the authors.

ABSTRACT Increasing demands for high-speed wireless communication have stimulated the development of novel optoelectrical devices. Typically, terahertz (THz) wave, is much advantageous because of its relatively high-resolution transportation and strong penetrability property. One of the electromagnetic devices, the antenna, plays a key role in future THz devices. However, there are few review publishments related to carbon-based THz microstrip antenna designs. In this article, we list the basic figure of merits for evaluating antennas. We also show the developing microstrip antenna structures. Importantly, we summarize the current progress of THz microstrip antennas using different dimensional carbon materials, such as carbon nanotubes, graphene, and carbon foams. This review will lay a solid foundation for carbon-based THz microstrip antenna design, and furthermore provide novel sights for other THz antenna designs.

INDEX TERMS Wireless communication, THz wave, carbon-based THz microstrip antenna.

I. INTRODUCTION

With the proposal and development of the fifth-generation mobile networks (5G), the demands for high-speed data communication have been highly increasing. terahertz (THz) band, acting as one of the possible solutions, has received great attention. THz wave, as a submillimeter-wave, ranges from 0.1 to 10 THz with a wavelength between 3 mm and 30 μm [1]. The generation of THz can be operated via bulk electro-optic rectification [2], surface field generation [3] and ultra-fast switching process of photoconductive emitters [4]. The frequency of THz wave lies between the top frequency of microwave and the bottom frequency of infrared (IR) frequency wave. In this circumstance, microwave belongs to the field of electricity that can be explained by the theory of electricity, while infrared waves belong to the field of optics, which can be explained by optical theory. Therefore, researchers try to take optics and electrics theories as references and explore their potential applications. Different from microwave and IR waves, the THz wave has its unique properties. Firstly, it can easily penetrate daily necessities such as clothes, paper, plastics without any attenuation. Secondly, the THz band has a shorter wavelength than the microwave, which can achieve high-resolution communication. Thirdly, the THz wave has a very low power level, non-ionizing detection process can be achieved. Applications upon THz waves have an unprecedented expansion in the decade of years, specifically covering medical imaging [4], agriculture and food detection [5], military radar [6], and especially wireless communication including photodetector [7]–[9] and antenna [10], [11].

The antenna is one device that can receive and transmit electromagnetic radio waves [12], and is usually divided into the horn [13], microstrip [14], dipole [15], bow-tie [16], Yagi-Uda [17] and lens antennas [18]. Different antennas have their distinctive structures and properties, and thus have corresponding applications. In the frequency of THz regime, antenna can be roughly divided into metallic antenna [19], dielectric antenna [20] and new-material antenna. As for the THz metallic antennas, most of them are radiated using copper material. Nevertheless, the designed copper-based antenna encounters low conductivity and low mobility problems [21]. Compared with copper, graphene acting as a typical two-dimensional carbon-based material has been applied for new material-based THz antenna [22]. The unique hexagonal planar structure of graphene promotes the inside carrier transfer,

This work is licensed under a Creative Commons Attribution-NonCommercial-NoDerivatives 4.0 License. For more information, see https://creativecommons.org/licenses/by-nc-nd/4.0/

which thus increases the mobility, as well as the conductivity of antennas [23]. After that, several simulations towards the electrical and magnetic properties of various dimensional carbon-based materials have been proposed and investigated via CST microwave studio or Ansys HFSS software for designing THz antennas.

In this paper, THz antennas applying carbon nanotubes (CNTs), or graphene will be presented. Except that, the advantages and disadvantages of multiple carbon materials will be discussed in detail. The structure of this paper is as follows: Section II focuses on a detailed introduction on several parameters related to the antenna. Section III presents some fundamental structural components of microstrip antennas, followed by the impact of various-shaped slots on the antenna performance. As the core part of this paper, Section IV describes the performance of THz microstrip antennas including 1D carbon structure achieved by CNTs and carbon nanofibers (CNFs), 2D carbon structure achieved by graphene, as well as 3D carbon structure achieved by carbon foams and 3D-graphene. Several physical antennas and simulated results are proposed and summarized. Finally, this review concludes by giving an outlook on THz microstrip antenna with different dimensional carbon materials in the abovementioned sections.

II. FIGURE OF MERITS

The properties of compact, broad impedance bandwidth and high radiation efficiency are main obstacles for researchers to utilize the THz band to design antennas. Therefore, it is crucial to find suitable standards to evaluate antenna performance. In this case, one particular antenna can be evaluated by some electromagnetic parameters including radiation pattern, directivity, gain, impedance, reflection coefficient, voltage standing wave ratio (VSWR) and scattering parameters. In this section, several basic concepts and equations used for describing the impacts and evaluating antenna performance are provided.

A. DIRECTIVITY, RADIATION EFFICIENCY AND GAIN

Directivity and radiation efficiency acts as the standard terminologies for antennas. [24] Directivity denotes the ratio of the antenna radiation intensity in a given direction to the averaged radiation intensity over all directions [25]. Radiation efficiency, also used as antenna efficiency, represents the transformation rate of radio frequency (RF) power accepted into radiated power [12].

Gain describes the degree to which the antenna converts input power into radio waves emitted in a particular direction based on a transmitting antenna or converts radio waves from a particular direction into electrical energy based on a receiving antenna [26]. It combines the directivity (D) and radiation efficiency (ε_r) parameter of one particular antenna by the equation:

$$G = D \cdot \varepsilon_r. \tag{1}$$

B. IMPEDANCE

Due to the wide use of impedance in different fields, there is no precise definition for antenna impedance. In this case, antenna impedance can be regarded as the resistance to a transmitted or received electrical signal in a particular antenna, which serves as a basic but crucial parameter of antenna performance evaluation.

C. RADIATION PATTERN

Radiation pattern, also known as gain pattern, refers to the visual scheme of how the antenna source and detector transmit and receive radio frequency energy [12]. The radiation pattern can be considered as a plot of gain regarding the direction change, which is divided into two-dimensional (2D) radiation patterns and three-dimensional (3D) radiation patterns (Fig. 1(a)). Among that, the radiation pattern is widely applied due to its straightforward. representation of the relationship between the antenna's main lobe and the sidelobe (Fig 1(b)). The main lobe represents the largest lobe area in the desired propagated direction and the side lobe is the lobe area in unwanted directions [24]. With a bigger the ratio of the main lobe and the side lobe area, antennas will show a higher working efficiency.

As shown in Fig. 1(c) and (d), two configurations also known as *H-plane* and *E-plane*, are measured. The *H-plane* stands for the horizontal plane which generally coincides with XY plane in normal coordinates or $\Phi = 90^\circ$ in spherical coordinates [12]. It can be easily used for measuring the radiation efficiency and the maximum directivity of the antenna. As for the *E-plane*, it represents the elevation plane where $\Phi = 0^\circ$ in spherical coordinates [12].

D. SCATTERING PARAMETERS AND REFLECTION COEFFICIENT

Scattering parameters (S-parameters) provide a relationship between the input and output power of different ports in the antenna structure, which can be measured using the port analysis method [26]. Among the scattering parameters, the absolute value of S_{11}, which stands for the amount of power reflected from the antenna, has become the main focus and is generally quoted by radio frequency engineers in most recent research papers. The absolute value of S_{11} can be calculated according to the following equation:

$$\begin{aligned} |S_{11}| &= \lim_{l\to\infty} \left| \frac{\left(Z_0^2 - Z_L^2\right)\sinh(\gamma l)}{2Z_L Z_0 \cosh(\gamma l) + \left(Z_L^2 + Z_0^2\right)\sinh(\gamma l)} \right| \\ &\approx \left| \frac{\left(Z_0^2 - Z_L^2\right)\exp(\gamma l)}{2Z_L Z_0 \exp(\gamma l) + \left(Z_L^2 + Z_0^2\right)\exp(\gamma l)} \right| \\ &= \left| \frac{(Z_0 - Z_L)(Z_0 + Z_L)}{2Z_L Z_0 + Z_L^2 + Z_0^2} \right| \\ &= \left| \frac{(Z_0 - Z_L)}{(Z_0 + Z_L)} \right| = |\Gamma| \end{aligned} \tag{2}$$

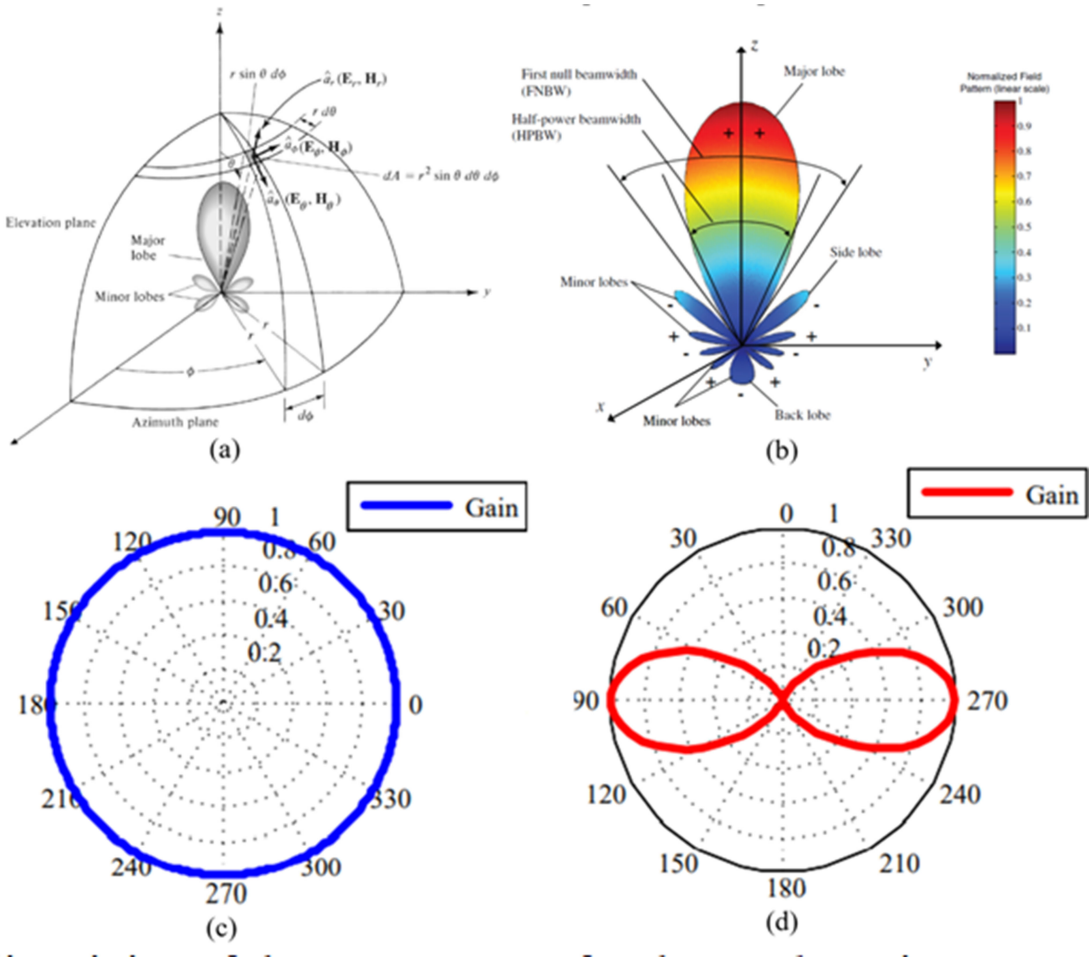

FIGURE 1. Schematic diagram of (a) Spherical Coordinates for antenna analysis. (b) Working pattern of an antenna. Reproduced from [[12], Copyright 2015, with the permission of IEEE. (c) The simulation of the H-plane radiation pattern in omni-direction. (d) The simulation of the E-plane radiation pattern in omni-direction. Reproduced from [[27], Copyright 2010, with the permission of IEEE.

where Z_L is the load impedance, Z_0 is the characteristic impedance and Γ is the reflection coefficient.

According to the (2), it can be seen that the absolute value of S_{11} and Γ are the same. Except that, reflection coefficient (Γ) can be quantized as the amplitude ratio of the reflected voltage (V^-) to that of the forward voltage (V^+) [12] by applying the below equation:

$$\Gamma = \frac{V^-}{V^+} = \frac{Z_L - Z_0}{Z_L + Z_0} \tag{3}$$

E. VOLTAGE STANDING WAVE RATIO

Voltage Standing Wave Ratio is usually abbreviated as VSWR, which varies by the reflection coefficient and reports the power reflected from the antenna [12]. VSWR can be calculated via the following formula:

$$VSWR = \frac{1 + |\Gamma|}{1 - |\Gamma|} \tag{4}$$

where Γ stands for the reflection coefficient. The antenna will perform better if it has a smaller value of VSWR, which means more power is delivered from the transmitter to the detector. As for an ideal THz antenna, the reflection coefficient is equal to 0 and the minimum value of VSWR can be achieved for 1.0.

E. RETURN LOSS

Return loss is correlated with the reflection coefficient (Γ) parameter and reveals the magnitude of the reflected wave [12]. In recent research, the return loss is mostly expressed as negative to express the loss. The bigger the absolute value of return loss is, the larger the antenna receives and the better the antenna detector performs consequently. The relationship between return loss and reflection coefficient is as followed:

$$\begin{aligned} Return\ Loss &= -20 \cdot \log(\Gamma) = -10 \cdot \log\left(\left|\frac{P_r}{P_i}\right|\right), \\ &= -20 \cdot \log\left(\left|\frac{V_r}{V_i}\right|\right) \end{aligned} \tag{5}$$

where P_r and V_r are the power and voltage of reflection, and P_i and V_i are the power and voltage of input. According to the above equation, it can be seen that the value of return loss

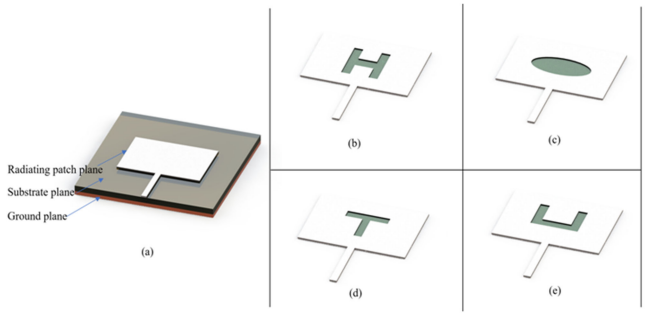

FIGURE 2. Schematics of the (a) Simple microstrip antenna structure. (b) H-shaped slot radiating patch plane. (c) Elliptical-shaped slot radiating patch plane. (d) T-shaped slot radiating patch plane. (e) U-shaped slot radiating patch plane.

will decrease with the increasing value of reflection coefficient (Γ).

III. STRUCTURE

Microstrip antennas, also referred to as the patch antenna, are preferred for easily integrated and fabricated, as well as low-cost characteristics [27]. It is composed of three fundamental planes: the substrate plane, the ground plane, and the radiating patch plane. Although there are many geometrical shapes designed and reported by RF researchers [23]–[29], rectangular substrate-based THz microstrip antenna is widely used in recent research. In this structure, the radiating patch plane is assembled on one side of the dielectric substrate plane and the ground plane is on the other side.

Some designed antenna structures are summarized in Table I (shown in the supporting information) [30]–[35]. In terms of the fabricated size of the microstrip antenna, there is a close relationship among the size of antenna, the resonant frequency, and the wavelength of THz wave: the total length of antenna is in inverse proportion to the resonant frequency and directly proportional to the wavelength. In this case, the higher the resonant frequency performs, the smaller the antenna can be made. Meanwhile, the length (L) of rectangular microstrip structure is around one-half wavelength in the dielectric medium, the width (W) controls the level of input impedance [41], and the thickness is mostly controlled under 200 micrometres.

Since the slot on the radiating patch plane has a crucial effect on the antenna performance, choosing the suitable shape of the slot patch layer is significant for researchers. As Fig. 2 shown, H-shaped, U-shaped, Elliptical-shaped, T-shaped, and some novel-shaped slots are mostly used in recent research.

According to the performance of different antennas, the slot-shaped antenna becomes more compact compared with antennas without slots. Meanwhile, with the improvement of inducing different shape slots, each of them has its own disadvantages. For instance, elliptical-slot hexagonal THz antenna performance better in accordance with gain, return loss, and VSWR and a higher resonant frequency at 1.400 THz, but offers lower directivity for the operating frequency below 0.85 THz compared with same size U-slot shaped antenna [37].

IV. MATERIAL

The selection of suitable materials is a significant step for designing a high-performance THz microstrip antenna. The frequency of resonance, relative permittivity, conductivity, and loss tangent acts as the leading criteria in material selection. Meanwhile, due to the special "sandwich-like" structure of the microstrip patch antenna detector, researchers need to consider not only the mentioned parameters of the materials, but also the compatibility between every structure plane. The radiating patch plane plays the most important role among the microstrip patch antenna structures. In terms of frequency in the THz range, copper is mostly used for metal patch THz antenna [42]. However, copper antenna has a relatively large energy loss during the propagation process and a decreased radiation efficiency due to the mobility and conductivity limitation of copper at THz frequency. Compared with copper THz antenna, carbon-based materials have been examined and had a satisfying performance for the THz regime [38]–[42], which makes it possible to apply this type of materials on designing THz antenna. In this section, different dimensional carbon-based materials are introduced in accordance with their performance on THz microstrip antenna. By summarizing the parameters and comparing, the advantages and disadvantages will be concluded.

A. ONE-DIMENSIONAL CARBON-BASED MATERIAL

CNTs are discovered by Sumio Iijima in 1991, which are rolled up into tubular structures by sp^2-bonded graphite sheets with nanometer diameter and large length ratio [48]. They can be divided into either single-walled carbon nanotubes (SWCNTs) and multi-walled carbon nanotubes (MWCNTs) generally, or zigzag CNT, armchair CNT, and chiral CNT for SWCNTs, and special type double-walled carbon nanotubes (DWCNTs) for MWCNTs in detail. Compared with MWCNTs, SWCNTs usually show higher electrical conductivity, better thermal conductivity, and smaller resistivity due to the unity of structure. Recent researches based on SWCNTs material focuses on applying dipole antenna, which has excellent performance through the sub-THz and THz frequency [44]–[48]. Only a limited number of researches simulated and fabricated SWCNTs microstrip antenna [49]–[52]: Mehdipour *et al.* [58] use SWCNTs composites and design a low-profile wideband microstrip-fed monopole antenna, which performs 2.6 dB/cm loss between 0.024–0.034 sub-THz region, and 0.94–2.24 dB peak gain. However, reported antennas meet low radiation efficiency associated with the loss challenge.

As for the application of MWCNTs, although they are highly disordered and contain many defects, some MWCNTs loaded microstrip THz antennas are invented. In 2009, Elwi *et al.* [59] apply inkjet printing technique on embedding purified MWCNTs in a sodium cholate composite thin film to create a patch antenna that performs nearly 45% more bandwidth and the same radiation pattern in contrast to copper patches

with identical antenna structure between 0-10 GHz sub-THz region. To shorten the microstrip line and detect less than millimetre wave, Thampy and Dhamodharan [60] designed an MWCNT loaded fluorine-doped tin oxide (FTO) based optical transparent patch antenna. This patch antenna has a great performance between 0.711–0.796 THz and achieves a broad impedance bandwidth of 11.33% and around 40% radiation efficiency. Nevertheless, the impedance mismatch challenge between MWCNTs and the doped materials still exists in this structure. Based on previous research, they designed another type of transparent antennas based on MWCNTs loaded indium-doped tin oxide (ITO) and titanium-doped tin oxide (TIO), which achieves −45.13 dB and −40.51dB return losses at 0.750 GHz and 46.13% and 61.01% radiation efficiency respectively [61].

Despite the defects of SWCNTs and MWCNTs, researchers try to combine them and produce nanotube bundles [57], [58] or sheets [59], [60], which can exhibit higher radiation efficiencies orders than individual CNTs antenna [66] and higher radiation efficiency with the increasing nanotube density of the bundle [67]. In 2004, Zhou *et al.* [68] propose a conductive CNTs sheet via polymer-printing technology and construct a polymer-CNTs based microstrip antenna, which achieves 5.6 dB gain and 0.9 Ω/square resistivities. To investigate the relationship between the antenna impedance and the density of SWCNTs, Mostofizadeh *et al.* [69] focused on the electrical properties of SWCNTs bundles. The results show that when the equivalent number density of SWCNTs is up to 10^4 CNTs/μm , the antenna can yield more than 90% radiation efficiency in THz regime between 1 THz and 50 THz. At the same time, the impedance of SWCNTs bundle decreases with the increasing number of SWCNTs, which thereby reduces the high resistive loss and kinetic inductance of SWCNTs. Combined with the performance and development of carbon nanotubes in the THz microstrip antenna, it is seen that CNTs can be utilized as a suitable alternative for copper patch antenna. In 2014, Keller *et al.* [70] fabricated a vertically aligned MWCNTS array sheet film by applying the chemical vapor deposition (CVD) technique and simulated a MWCNT-based sheet microstrip antenna. The result shows that the performance of the MWCNTs-based sheet patch antenna can be affected by the thickness of the CNT sheet. Compared with 0.5 *um*-thick CNT sheet radiating layer, 5 *um*-thick exhibits a much larger reflection coefficient and performs a 5.5 *dB* higher gain. In addition, they found that the angle between the fabricated CNT alignment and the E-plane of the antenna could also affect the final performance of the antenna: If the alignment is fabricated orthogonally to the E-plane, there is an over 8 *dB* gain reduction realized. Nevertheless, the performance of CNT antennas is still slightly inferior compared with copper microstrip antennas with the same structure even though 5 *um*-thick CNT sheet has the best performance among CNT antennas with different thicknesses. The 5 *um*-thick CNT sheet antenna achieves 2.1 *dBi* total gain contrast with 5.6 *dBi* of copper patch antenna. Researchers inferred the around 3.5 *dBi* reduction ascribed to the material restriction.

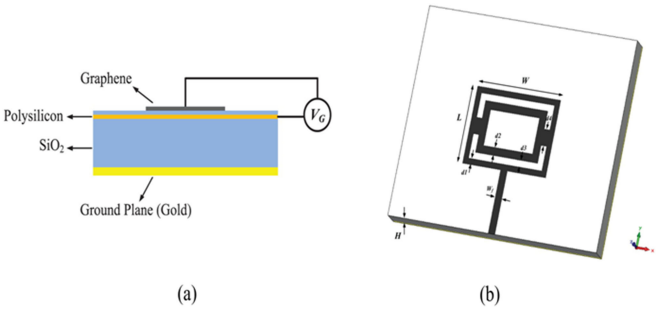

FIGURE 3. Schematic diagram of a Rectangular Double-Ring Nanoribbon Graphene-Based Antenna. (a) Longitudinal section topology. (b) Top view antenna structure. Reproduced from [76], Copyright 2019, with the permission of IEEE.

CNFs (diameter 3–100 nm; length 0.1–1000 μm) are composed of cylindrical or conical wrapped graphene layers [71]. Compared with carbon nanotubes, carbon nanofibers have similar flexibility, stability, and conductivity. Moreover, due to different shapes formed of the stacked graphene layers inside CNFs, there are more edge sites created on the outer surface, which improves the charge transport process in the structure [72]. In the past few years, most research has applied CNFs in the field of electrocatalysis [73], gas storage [74] and probe tips [75]. The use of CNFs composite has been investigated for building[76] antennas and RF circuit [52], [64] in recent years. Lee, *et al.* [75] fabricate CNF films via electrospinning technique and the result shows that relatively thick CNF ($\sim$430 μm) will perform an acceptable electric conductivity ($\varepsilon = 6.30$) and electric permittivity ($\sigma = 0.75$S/m) at 0.5 GHz, which makes it possible to use the composite of CNFs to produce an antenna related device i.e., signal attenuator [77].

B. TWO-DIMENSIONAL CARBON-BASED MATERIAL

In terms of two-dimensional carbon-based material, the most typical and basic type is graphene, which was discovered by Novoselov *et al.* [78] in 2004 via the micro-mechanical cleavage method. Since it can be considered as a planar sheet of carbon atoms that bonded together by sp^2 hybrids in a hexagonal lattice [69], the properties of graphene can be fully described by its surface conductivity σ, expressed by the Kubos formula [79]. Considering the advantages of high conductivity, low channel electrical resistance, and also high mobility [21], graphene has been currently drawn exceptional attention applied for electromagnetic (EM) applications such as wireless communication. Recently, several publications have focused on the electric properties of graphene in the THz regime [68]–[72] and utilized graphene as the antenna patch plane material. For instance, in 2012, Llatser *et al.* [85] simulated a simple graphene-based nano-patch antenna using a 5×0.5 μm graphene patch plane.

As Fig. 3 shown, the patch plane is fabricated by means of a pin feed technique, which locates on the different locations of a silicon substrate with a dimension of 6 × 6× 1 μm^3. In this research, graphene-based patch plane antenna

accomplishes a 0.5 THz resonant frequency and performs nearly identical radiation pattern plots in accordance with the equivalent metallic antenna, following with the theoretical hypothesis that graphene-based patch antenna can resonate in the THz band. In 2017, Azizi *et al.* [86] design a square graphene-based radiating patch plane microstrip THz antenna on a perfect electric conductor (PEC) ground plane with a dimension of $119.54 \times 151.5 \times 15\ \mu m^3$. By simulating a planar patch plane with monoatomic graphene, this antenna exhibits a -29 dB peak return loss and approximately 7.16 dB gain at a 0.7 THz resonant compared with -15 dB return loss and 5.73 dB gain performance of copper patch antenna.

However, the THz microstrip antenna proposed to meet either large in size or narrow bandwidth challenge [35]. In addition to the previously mentioned use of slots on the surface of the radiating patch plane, inside structure changes and material selection of graphene-based microstrip patch antennas are proposed in some studies. To increase the antenna bandwidth and solve impedance mismatching and low optimal efficiency problem, Nickpay *et al.* [76] designed a graphene-based microstrip antenna with double-ring nanoribbon.

As Fig. 3(a) shown, this novel antenna uses silicon dioxide (SiO_2) as substrate and gold as ground plane which has a dimension of $93 \times 120 \times 25\ \mu m^3$ with a total thickness of 3.4 nm graphene layers. The results show it can achieve 26% impedance bandwidth, 24 dB return loss, 44% average radiation efficiency and 2.45 dB gain with a 1 THz center frequency. In 2021, Shamim *et al.* [37] demonstrated that the permittivity or dielectric constant of the substrate material also directly affects the size and performance of the antenna. They designed a rectangular graphene-based wideband microstrip antenna using Arlon AD 1000 with 10.2 relative permittivity and 0.0023 loss tangent as substrate, and copper as ground plane material. The simulated antenna occupies a dimension of $120 \times 120 \times 45\ \mu m^3$, which offers a 37.50 % impedance bandwidth with -59.67 dB return loss, 6.60 dB directivity and 1.007 VSWR at 0.72 THz resonant frequency.

C. THREE-DIMENSIONAL CARBON-BASED MATERIAL

Due to the limitation of size and fabricated technologies, few researchers have applied three-dimensional carbon-based material on fabricating antennas. However, trials on this type of material performance in THz band regime are still ongoing. Some typical types of three-dimensional carbon-based material include carbon foam and 3D graphene structure. Carbon foam has attracted attention due to its unique porous conductive network inside the structure, which contains valid space for transmitting and absorbing electromagnetic wave radiation. In 2017, Letellier *et al.* [87] measure the relationship between the structural and electromagnetic properties of different types of simulated carbon foams. The result shows that carbon modelled cellular vitreous (CVC) foam can perform in a broad frequency extent from 20 Hz to 250 THz, which confirms the possibility of using carbon foams at the frequency of the THz regime. At present, most of the current research applies the high absorption characteristics of carbon foam to THz waves in the field of electromagnetic interference shielding. In terms of the three-dimensional graphene material, it has been proposed and applied to THz-related applications. Different from the typical 2D graphene plane model, 3D graphene is configured into a complex pillars structure, which not only retains the electrical advantages of graphene, but only solves the restacking problems of 2D graphene. In 2016, Song *et al.* [88] propose the transformation of graphene structure from 2D to 3D and demonstrate that the structure change excites the high order plasmonic modes which contributes to overcome the interference occurring in flat graphene structures. One of expected structure models of 3D graphene is presented in Fig. 4(a).

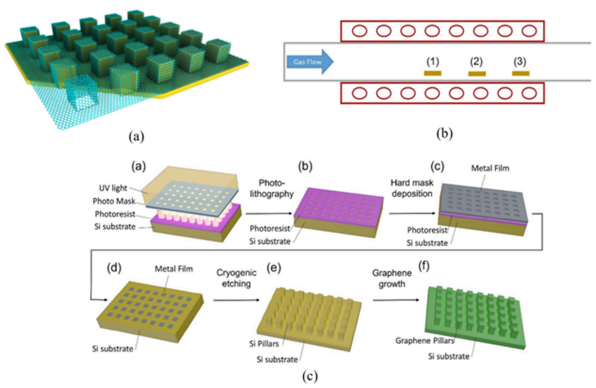

FIGURE 4. (a) Expected schematic diagram of 3D graphene pillar array. (b) CVD technique utilized for the growth of graphene samples. (c) Fabrication process of graphene pillars on intrinsic silicon substrate. Reproduced from [88], Copyright 2017, with the permission of IEEE.

As shown in Fig 4(b), 3D graphene pillar array is fabricated utilizing the chemical vapour dynamics technique by growing controllable graphene films on prefabricated silicon pillars, which firstly achieves a high order plasmonic mode excitation inside graphene structure. These publication results lay a foundation for the study for controlling THz radiation. In 2020, Asgari *et al.* [89] proposed a three-dimensional (3D) graphene intrinsically chiral meta-structure which can be used for antenna-related biosensing applications. As shown in Fig. 5(b), a thin cross-shaped graphene strips with an area dimension of $20 \times 5\ \mu m^2$ and 0.335 nm thickness is deposited on the alumina layer. The simulation results show that this graphene chiral structure has a good performance under THz waves of 1.48, 2.46 THz and as high as 0.96 THz refractive index unit is obtained between 0.5–3.5 THz region. This structure design contributes the potential for utilizing this structure design as a THz biosensor.

SUMMARY AND PROSPECTS

In this paper, the applications of multi-dimensional carbon-based materials on THz and sub-THz microstrip antennas are discussed. It is obvious and undeniable that carbon nanotubes and graphene have become the main research objects on building microstrip antennas and testing their performance. Among these carbon-based materials, several challenges and efforts

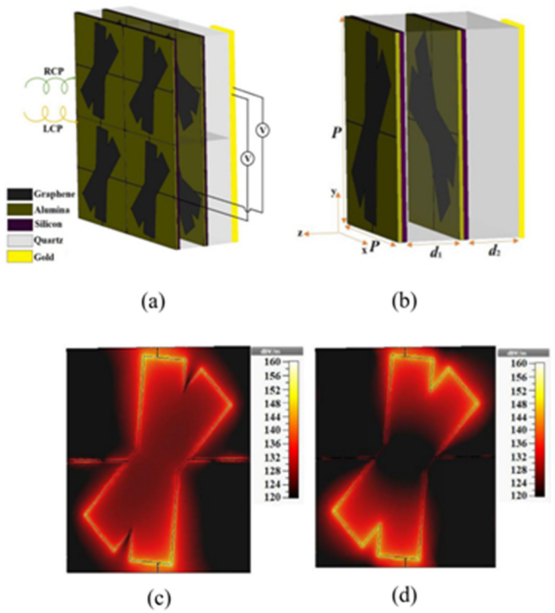

FIGURE 5. Schematics of the (a) periodic, (b) unit cell of the bi-layer 3D THz graphene chiral structure; the electric field distributions of the proposed structure at (c) 1.48 THz, (d) 2.46 THz. Reproduced from [89], Copyright 2020, with the permission of IEEE.

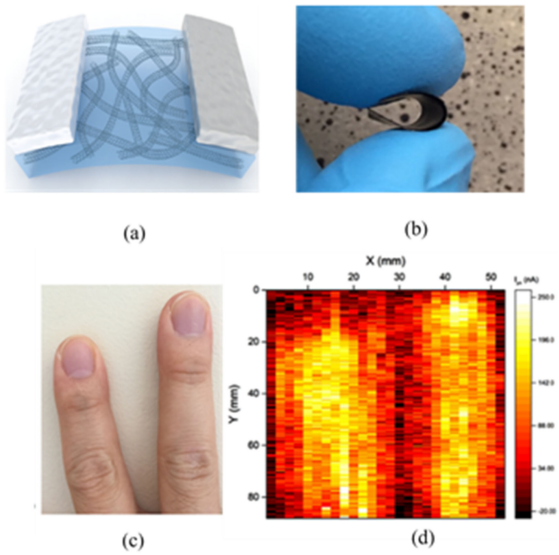

FIGURE 6. Schematics of (a) the PTE detector (the upper two columns are the Al/Ti electrodes and the below plat is the PVA/CNTs thin film). (b) Physical photos of the flexible PVA/CNT thin fims. (c) Fingers placement. (d) Thermal imaging result. Reproduced from [93], Copyright 2018.

have been proposed during the research. First of all, narrow impedance bandwidth is the most common problem met in recent THz antenna research [89]. Although various-shaped slots have been proposed and applied to solve this problem and improve the antenna's directivity and gain, the mismatch loss between the substrate plane and the radiation plane still exists [36]. Secondly, controlling the size of the microstrip antenna is another existing challenge [90]. Several trials including adding additional materials such as polymers [91] or forming carbon bundles [67] via mixing different carbon materials have been investigated to increase the unit density of radiating planes. However, the interaction inside the plane may influence the original carbon-based structure i.e., flat to curved, and therefore have an indirect impact on conductivity and permittivity parameters. Thirdly, the intrinsic characteristics of carbon-based material also limit the performance of designed microstrip antennas. For instance, restacking problems of graphene [92] planes will directly affect the planar conductivity of the antenna, which increases the power dissipation and eventually reduces the antenna efficiency. Summarily, future development should target for microfabricate a compact wide-band carbon-based THz microstrip antenna with high radiation efficiency, low impedance, high gain Further prospective includes designing new shaped slots, selecting more suitable substrate plane materials, and introducing novel composites or bundles.

As for our group previous work towards Terahertz spectral region, photo thermoelectric (PTE) detectors have been deeply researched. In 2018, Zhang [93] applied poly-(vinyl alcohol) (PVA) and CNTs nanocomposites and designed a wearable device according to the PTE effect. As Fig. 6(a) shown, this device is fabricated by bonding a PVA/CNT composite thin film on the surface of two aluminum plates and using Al/Ti columns as electrodes. The results demonstrate that 30 $wt\%$ CNT contained device performs a $1.6\times10^{6} cm\ Hz^{1/2}\ W^{-1}$ with a 3.5 mm bending radius, and 60 $wt\%$ CNT contained device performs a 4.9×10^{6} cm $Hz^{1/2}$ W^{-1} with a 15 mm bending radius. Besides, he morphology of fingers (shown in Fig. 6(c), (d)) and obtained a clear imaging figure. The performance of PVA /CNTs composites-based PTE detector provides a great potential for utilizing it in the field of wearable flexible health monitoring devices i.e., cancer imaging.

Conflict of interest: There is no conflict of interest among authors.

REFERENCES

[1] D. Dragoman and M. Dragoman, "Terahertz fields and applications," *Prog. Quantum Electron.*, vol. 28, no. 1, pp. 1–66, 2004, doi: 10.1016/S0079-6727(03)00058-2.

[2] L. Xu, X. C. Zhang, and D. H. Auston, "Terahertz beam generation by femtosecond optical pulses in electro-optic materials," *Appl. Phys. Lett.*, vol. 61, no. 15, pp. 1784–1786, 1992, doi: 10.1063/1.108426.

[3] A. G. Davies, E. H. Linfield, and M. B. Johnston, "The development of terahertz sources and their applications," *Phys. Med. Biol.*, vol. 47, no. 21, pp. 3679–3689, 2002, doi: 10.1088/0031-9155/47/21/302.

[4] A. G. Davies, A. D. Burnett, W. Fan, E. H. Linfield, and J. E. Cunningham, "Terahertz spectroscopy of explosives and drugs," *Mater. Today*, vol. 11, no. 3, pp. 18–26, 2008, doi: 10.1016/S1369-7021(08)70016-6.

[5] J. Qin, Y. Ying, and L. Xie, "The detection of agricultural products and food using terahertz spectroscopy: A review," *Appl. Spectrosc. Rev.*, vol. 48, no. 6, pp. 439–457, 2013, doi: 10.1080/05704928.2012.745418.

[6] S. Ergün and S. Sönmez, "Terahertz technology for military applications," *J. Mil. Inf. Sci.*, vol. 3, no. 1, PP. 13-16, 2015, doi: 10.17858/jmisci.58124.

[7] M. Zhang and J. T. W. Yeow, "A flexible, scalable, and self-powered mid-infrared detector based on transparent PEDOT: PSS/graphene composite," *Carbon N. Y.*, vol. 156, pp. 339–345, 2020, doi: 10.1016/j.carbon.2019.09.062.

[8] J. Wang, Z. Xie, and J. T. W. Yeow, "Two-dimensional materials applied for room-temperature thermoelectric photodetectors," *Mater. Res. Express*, vol. 7, no. 11, 2020, doi: 10.1088/2053-1591/abc6cc.

[9] M. Zhang, D. Ban, C. Xu, and J. T. W. Yeow, "Large-area and broadband thermoelectric infrared detection in a carbon nanotube blackbody absorber," *ACS Nano*, vol. 13, no. 11, pp. 13285–13292, 2019, doi: 10.1021/acsnano.9b06332.

[10] Y. Wang *et al.*, "Terahertz photodetector based on double-walled carbon nanotube macrobundle–metal contacts," *Opt. Express*, vol. 23, no. 10, 2015, Art. no. 13348, doi: 10.1364/oe.23.013348.

[11] P. H. Siegel, P. de Maagt, and A. I. Zaghloul, "Antennas for terahertz applications," pp. 2383–2386, 2008, doi: 10.1109/aps.2006.1711074.

[12] C. A. Balanis, *Antenna Theory: Analysis and Design*, 4th ed. Hoboken, NJ, USA: Wiley, 2015.

[13] E. Crystal and E. Structure, "Terahertz horn antenna based on hollow-core," *IEEE Trans. Antennas Propag.*, vol. 60, no. 12, pp. 5557–5563, Dec. 2012.

[14] K. R. Jha and G. Singh, "Analysis and design of terahertz microstrip antenna on photonic bandgap material," *J. Comput. Electron.*, vol. 11, no. 4, pp. 364–373, 2012, doi: 10.1007/s10825-012-0416-9.

[15] G. Q. He *et al.*, "Reconfigurable terahertz dipole antenna with integrated graphene sheets," in *Proc. Int. Conf. Microw. Millim. Wave Technol.*, 2020, pp. 2020–2022, doi: 10.1109/ICMMT49418.2020.9386643.

[16] M. Runge, D. Engel, M. Schneider, K. Reimann, M. Woerner, and T. Elsaesser, "Spatial distribution of electric-field enhancement across the gap of terahertz bow-tie antennas," *Opt. Express*, vol. 28, no. 17, 2020, Art. no. 24389, doi: 10.1364/oe.399462.

[17] S. Poorgholam-Khanjari, F. B. Zarrabi, and S. Jarchi, "Compact and wide-band quasi yagi-uda antenna based on periodic grating ground and coupling method in terahertz regime," *Optik (Stuttg),* vol. 203, 2020, Art. no. 163990, doi: 10.1016/j.ijleo.2019.163990.

[18] C. Apriono and F. Ulfah, "Radiation performances of side reduced terahertz dielectric silicon lens antenna," in *Proc. 12th Int. Conf. Inf. Technol. Elect. Eng.*, 2020, pp. 1–4, doi: 10.1109/ICITEE49829.2020.9271706.

[19] G. M. Rebeiz, "Millimeter-wave and terahertz integrated circuit antennas," *Proc. IEEE*, vol. 80, no. 11, pp. 1748–1770, Nov. 1992, doi: 10.1109/5.175253.

[20] J. R. Bray and L. Roy, "Physical optics simulation of electrically small substrate lens antennas," in *Proc. Can. Conf. Elect. Comput. Eng.*, 1998, pp. 814–817, doi: 10.1109/ccece.1998.685622.

[21] S. M and G. M. M, "Performance predictions of slotted graphene patch antenna for multi-band operation in terahertz regime," *Optik (Stuttg),* vol. 204, 2020, Art. no. 164223, doi: 10.1016/j.ijleo.2020.164223.

[22] S. Abadal, S. E. Hosseininejad, A. Cabellos-Aparicio, and E. Alarcón, "Graphene-based terahertz antennas for area-constrained applications," in *Proc. 40th Int. Conf. Telecommun. Signal Process.*, 2017, pp. 817–820, doi: 10.1109/TSP.2017.8076102.

[23] U. G. H. Surface, "Reconfigurable terahertz leaky-wave antenna," *IEEE Trans. Nanotechnol.*, vol. 14, no. 1, pp. 62–69, Jan. 2015.

[24] *IEEE Standard Definitions of Terms for Antennas*, Anon, Piscataway, NJ, USA: IEEE, 1983.

[25] C. A. Balanis, "Antenna theory: A review," *Proc. IEEE*, vol. 80, no. 1, pp. 7–23, Jan. 1992, doi: 10.1109/5.119564.

[26] W. L. S. and G. A. Thiele, *Antenna Theory and Design*. Hoboken, NJ, USA: Wiley, 2012.

[27] S. Ghosh, S. Das, D. Samantaray, and S. Bhattacharyya, "Meander-line-based defected ground microstrip antenna slotted with split-ring resonator for terahertz range," *Eng. Rep.*, vol. 2, no. 1, pp. 1–9, 2020, doi: 10.1002/eng2.12088.

[28] S. Singhal and Jaiverdhan, "Hexagonal fractal antenna for super wideband terahertz applications," *Optik (Stuttg),* vol. 206, 2020, Art. no. 163615, doi: 10.1016/j.ijleo.2019.163615.

[29] S. Das, D. Mitra, and S. R. Bhadra Chaudhuri, "Fractal loaded circular patch antenna for super wide band operation in THz frequency region," *Optik (Stuttg),* vol. 226, no. P2, 2021, Art. no. 165528, doi: 10.1016/j.ijleo.2020.165528.

[30] A. Singh and S. Singh, "A trapezoidal microstrip patch antenna on photonic crystal substrate for high speed THz applications," *Photon. Nanostructures - Fundam. Appl.*, vol. 14, pp. 52–62, 2015, doi: 10.1016/j.photonics.2015.01.003.

[31] D. P. Cerkoney *et al.*, "Cavity mode enhancement of terahertz emission from equilateral triangular microstrip antennas of the high-T c superconductor Bi2Sr2CaCu2O8 + δ," *J. Phys. Condens. Matter*, vol. 29, no. 1, 2017, doi: 10.1088/0953-8984/29/1/015601.

[32] U. Keshwala, K. Ray, and S. Rawat, "Ultra-wideband mushroom shaped half-sinusoidal antenna for THz applications," *Optik (Stuttg),* vol. 228, 2021, Art. no. 166156, doi: 10.1016/j.ijleo.2020.166156.

[33] L. Guo, F. Huang, and X. Tang, "A novel integrated MEMS helix antenna for terahertz applications," *Optik (Stuttg),* vol. 125, no. 1, pp. 101–103, 2014, doi: 10.1016/j.ijleo.2013.06.016.

[34] M. Younssi, A. Jaoujal, Y. Diallo, A. E. Moussaoui, and N. Aknin, "Study of a microstrip antenna with and without superstrate for terahertz frequency," *Int. J. Innov. Appl. Stud.*, vol. 2, no. 4, pp. 369–371, 2013.

[35] S. M. Shamim, M. S. Uddin, M. R. Hasan, and M. Samad, "Design and implementation of miniaturized wideband microstrip patch antenna for high-speed terahertz applications," *J. Comput. Electron.*, vol. 20, no. 1, pp. 604–610, 2021, doi: 10.1007/s10825-020-01587-2.

[36] R. K. Kushwaha, P. Karuppanan, and L. D. Malviya, "Design and analysis of novel microstrip patch antenna on photonic crystal in THz," *Phys. B Condens. Matter*, vol. 545, pp. 107–112, 2018, doi: 10.1016/j.physb.2018.05.045.

[37] S. M. Shamim, S. Das, M. A. Hossain, and B. T. P. Madhav, "Investigations on graphene-based ultra-wideband (UWB) microstrip patch antennas for terahertz (THz) applications," *Plasmonics*, vol. 16, no. 5, pp. 1623–1631, 2021, doi: 10.1007/s11468-021-01423-8.

[38] P. Yin, L. Xu, and X. Bai, "Design of wide-band terahertz slotted antenna in CMOS," vol. 2019, p. 211, 2019, doi: 10.1117/12.2543765.

[39] C. Occhiuzzi, S. Caizzone, and G. Marrocco, "Passive UHF RFID antennas for sensing applications: Principles, methods, and classifcations," *IEEE Antennas Propag. Mag.*, vol. 55, no. 6, pp. 14–34, Dec. 2013, doi: 10.1109/MAP.2013.6781700.

[40] A. S. Dhillon, D. Mittal, and E. Sidhu, "THz rectangular microstrip patch antenna employing polyimide substrate for video rate imaging and homeland defence applications," *Optik (Stuttg),* vol. 144, pp. 634–641, 2017, doi: 10.1016/j.ijleo.2017.07.018.

[41] R. Mishra, "An overview of microstrip," *Int. J. Technol. Innov. Res.*, vol. 21, no. 2, pp. 1–17, 2016, doi: 10.5281/zenodo.161524.

[42] S. Dash and A. Patnaik, "Material selection for THz antennas," *Microw. Opt. Technol. Lett.*, vol. 60, no. 5, pp. 1183–1187, 2018, doi: 10.1002/mop.31127.

[43] R. R. Hartmann, J. Kono, and M. E. Portnoi, "Terahertz science and technology of carbon nanomaterials," *Nanotechnology*, vol. 25, no. 32, 2014, doi: 10.1088/0957-4484/25/32/322001.

[44] G. Y. Slepyan, M. V. Shuba, S. A. Maksimenko, C. Thomsen, and A. Lakhtakia, "Terahertz conductivity peak in composite materials containing carbon nanotubes: Theory and interpretation of experiment," *Phys. Rev. B - Condens. Matter Mater. Phys.*, vol. 81, no. 20, pp. 1–6, 2010, doi: 10.1103/PhysRevB.81.205423.

[45] X. He *et al.*, "Carbon nanotube terahertz detector," *Nano Lett.*, vol. 14, no. 7, pp. 3953–3958, 2014, doi: 10.1021/nl5012678.

[46] S. S. Efazat, R. Basiri, and S. V. Al-Din Makki, "The gain enhancement of a graphene loaded reconfigurable antenna with non-uniform metasurface in terahertz band," *Optik (Stuttg)*, vol. 183, pp. 1179–1190, 2019, doi: 10.1016/j.ijleo.2019.02.034.

[47] M. Bazgir, M. Naser-Moghadasi, F. B. Zarrabi, A. S. Arezomand, and S. Heydari, "Nano particle implementation in nano loop antenna for energy harvesting application and light trapping," *Optik (Stuttg),* vol. 132, pp. 127–133, 2017, doi: 10.1016/j.ijleo.2016.12.033.

[48] Iijima, S., "Helical microtubules of graphitic carbon," *Nature*, vol. 354, no. 6348, pp. 737–740, 1991.

[49] M. F. Pantoja, D. H. Werner, P. L. Werner, and A. R. Bretones, "TDIE modeling of carbon nanotube dipoles at microwave and terahertz bands," *IEEE Antennas Wireless Propag. Lett.*, vol. 9, no. 2, pp. 32–35, 2010, doi: 10.1109/LAWP.2010.2041627.

[50] G. W. Hanson, "Fundamental transmitting properties of carbon nanotube antennas," *IEEE Antennas Propag.*, vol. 53, no. 11, pp. 247–250, Nov. 2005, doi: 10.1109/APS.2005.1552484.

[51] J. Hao and G. W. Hanson, "Infrared and optical properties of carbon nanotube dipole antennas," *IEEE Trans. Nanotechnol.*, vol. 5, no. 6, pp. 766–775, Nov. 2006, doi: 10.1109/TNANO.2006.883475.

[52] Y. Wang, Q. Wu, W. Shi, X. He, X. Sun, and T. Gui, "Radiation properties of carbon nanotubes antenna at terahertz/infrared range," *Int. J. Infrared Millimeter Waves*, vol. 29, no. 1, pp. 35–42, 2008, doi: 10.1007/s10762-007-9306-9.

[53] W. Yue, W. Qun, H. Xun-Jun, Z. Shao-Qing, and Z. Lei-Lei, "Terahertz radiation from armchair carbon nanotube dipole antenna," *Chin. Phys. B*, vol. 18, no. 5, pp. 1801–1806, 2009, doi: 10.1088/1674-1056/18/5/014.

[54] Y. N. Jurn, M. F. Malek, W. W. Liu, and H. K. Hoomod, "Investigation of single-wall carbon nanotubes at THz antenna," in *Proc. 2nd Int. Conf. Electron. Des. ICED*, 2011, pp. 415–420, doi: 10.1109/ICED.2014.7015841.

[55] M. Muthee and S. K. Yngvesson, "Terahertz radiation from antenna-coupled single walled carbon nanotubes," in *Proc. 36th Int. Conf. Infrared, Millimeter Terahertz Waves*, 2011, pp. 6–7, doi: 10.1109/irmmw-THz.2011.6105081.

[56] R. Verma *et al.*, "Carbon nanotube-based microstrip antenna gas sensor," in *Proc. Midwest Symp. Circuits Syst.*, 2013, pp. 724–727, doi: 10.1109/MWSCAS.2013.6674751.

[57] S. Kumar, N. Kamaraju, B. Karthikeyan, M. Tondusson, E. Freysz, and A. K. Sood, "Terahertz spectroscopy of single-walled carbon nanotubes in a polymer film: Observation of low-frequency phonons," *J. Phys. Chem. C*, vol. 114, no. 29, pp. 12446–12450, 2010, doi: 10.1021/jp103105h.

[58] A. Mehdipour, A. R. Sebak, C. W. Trueman, I. D. Rosca, and S. V Hoa, "29th national radio science conference psatri, king saud university, riyadh11421, Saudi Arabia 29th national radio science conference," pp. 1–8, 2012.

[59] T. A. Elwi, H. M. Al-Rizzo, D. G. Rucker, E. Dervishi, Z. Li, and A. S. Biris, "Multi-walled carbon nanotube-based RF antennas," *Nanotechnology*, vol. 21, no. 4, 2010, doi: 10.1088/0957-4484/21/4/045301.

[60] A. S. Thampy and S. K. Dhamodharan, "Performance analysis of MWCNT loaded fluorinedoped tin oxide based optically transparent terahertz patch antenna," in *Proc. IEEE Asia-Pacific Conf. Appl. Electromagn.*, 2015, pp. 142–145, doi: 10.1109/APACE.2014.7043763.

[61] A. S. Thampy and S. K. Dhamodharan, "Performance analysis and comparison of MWCNT loaded ITO and TIO based optically transparent patch antennas for terahertz communications," *Phys. E Low-Dimensional Syst. Nanostructures*, vol. 78, pp. 123–129, 2016, doi: 10.1016/j.physe.2015.11.030.

[62] E. Amram Bengio *et al.*, "High efficiency carbon nanotube thread antennas," *Appl. Phys. Lett.*, vol. 111, no. 16, 2017, doi: 10.1063/1.4991822.

[63] H. Arun, "Advancements in the use of carbon nanotubes for antenna realization," *AEU - Int. J. Electron. Commun.*, vol. 136, 2021, Art. no. 153753, doi: 10.1016/j.aeue.2021.153753.

[64] K. S. Chaya Devi, B. Angadi, and H. M. Mahesh, "Multiwalled carbon nanotube-based patch antenna for bandwidth enhancement," *Mater. Sci. Eng. B Solid-State Mater. Adv. Technol.*, vol. 224, pp. 56–60, 2017, doi: 10.1016/j.mseb.2017.07.005.

[65] J. A. Berres and G. W. Hanson, "z," vol. 59, no. 8, pp. 3098–3103, 2011.

[66] Y. Huang, W. Y. Yin, and Q. H. Liu, "Performance prediction of carbon nanotube bundle dipole antennas," *IEEE Trans. Nanotechnol.*, vol. 7, no. 3, pp. 331–337, May 2008, doi: 10.1109/TNANO.2007.915017.

[67] S. Choi and K. Sarabandi, "Performance assessment of bundled carbon nanotube for antenna applications at terahertz frequencies and higher," *IEEE Trans. Antennas Propag.*, vol. 59, no. 3, pp. 802–809, Mar. 2011, doi: 10.1109/TAP.2010.2103023.

[68] Y. Zhou, Y. Bayram, F. Du, L. Dai, and J. L. Volakis, "Polymer-carbon nanotube sheets for conformal load bearing antennas," *IEEE Trans. Antennas Propag.*, vol. 58, no. 7, pp. 2169–2175, Jul. 2010, doi: 10.1109/TAP.2010.2048852.

[69] A. Mostofizadeh, Y. Li, B. Song, and Y. Huang, "Synthesis, properties, and applications of low-dimensional carbon-related nanomaterials," *J. Nanomater.*, vol. 2011, 2011, doi: 10.1155/2011/685081.

[70] S. D. Keller, A. I. Zaghloul, V. Shanov, M. J. Schulz, D. B. Mast, and N. T. Alvarez, "Radiation performance of polarization selective carbon nanotube sheet patch antennas," *IEEE Trans. Antennas Propag.*, vol. 62, no. 1, pp. 48–55, Jan. 2014, doi: 10.1109/TAP.2013.2287272.

[71] J. Huang, Y. Liu, and T. You, "Carbon nanofiber based electrochemical biosensors: A review," *Anal. Methods*, vol. 2, no. 3, pp. 202–211, 2010, doi: 10.1039/b9ay00312f.

[72] K. K. Karuppanan, M. K. Panthalingal, and P. Biji, "Nanoscale, catalyst support materials for proton-exchange membrane fuel cells," in *Handbook of Nanomaterials for Industrial Applications*, Jan. 2018, pp. 468–495, doi: 10.1016/B978-0-12-813351-4.00027-4.

[73] D. J. Browning, M. L. Gerrard, J. B. Lakeman, I. M. Mellor, R. J. Mortimer, and M. C. Turpin, "Studies into the storage of hydrogen in carbon nanofibers: Proposal of a possible reaction mechanism," *Nano Lett.*, vol. 2, no. 3, pp. 201–205, 2002, doi: 10.1021/nl015576g.

[74] H. Cui, S. V. Kalinin, X. Yang, and D. H. Lowndest, "Growth of carbon nanofibers on tipless cantilevers for high resolution topography and magnetic force imaging," *Nano Lett.*, vol. 4, no. 11, pp. 2157–2161, 2004, doi: 10.1021/nl048740j.

[75] H. J. Lee, J. H. Jeong, and B. H. Kim, "Microwave transmission characteristics of carbon nanofiber films with different micrometer-scale thickness," *Carbon N.Y.*, vol. 173, pp. 419–426, 2021, doi: 10.1016/j.carbon.2020.11.020.

[76] M. R. Nickpay, M. Danaie, and A. Shahzadi, "Wideband rectangular double-ring nanoribbon graphene-based antenna for terahertz communications," *IETE J. Res.*, pp. 1–10, 2019, doi: 10.1080/03772063.2019.1661801.

[77] A. Das, C. M. Megaridis, L. Liu, T. Wang, and A. Biswas, "Design and synthesis of superhydrophobic carbon nanofiber composite coatings for terahertz frequency shielding and attenuation," *Appl. Phys. Lett.*, vol. 98, no. 17, pp. 1–4, 2011, doi: 10.1063/1.3583523.

[78] K. S. Novoselov *et al.*, "Electric field in atomically thin carbon films," *Science*, vol. 306, no. 5696, pp. 666–669, Oct. 2004, doi: 10.1126/SCIENCE.1102896/SUPPL_FILE/NOVOSELOV.SOM.PDF.

[79] E. G. Mishchenko, "Minimal conductivity in graphene: Interaction corrections and ultraviolet anomaly," *EPL*, vol. 83, no. 1, 2008, doi: 10.1209/0295-5075/83/17005.

[80] I. Llatser, C. Kremers, A. Cabellos-Aparicio, J. M. Jornet, E. Alarcón, and D. N. Chigrin, "Graphene-based nano-patch antenna for terahertz radiation," *Photon. Nanostructures - Fundam. Appl.*, vol. 10, no. 4, pp. 353–358, 2012, doi: 10.1016/j.photonics.2012.05.011.

[81] C. J. Docherty and M. B. Johnston, "Terahertz properties of graphene," *J. Infrared, Millimeter, Terahertz Waves*, vol. 33, no. 8, pp. 797–815, 2012, doi: 10.1007/s10762-012-9913-y.

[82] P. Tassin, T. Koschny, and C. M. Soukoulis, "Graphene for terahertz applications," *Science*, vol. 341, no. 6146, pp. 620–621, 2013, doi: 10.1126/science.1242253.

[83] M. Hasan, S. Arezoomandan, H. Condori, and B. Sensale-Rodriguez, "Graphene terahertz devices for communications applications," *Nano Commun. Netw.*, vol. 10, pp. 68–78, 2016, doi: 10.1016/j.nancom.2016.07.011.

[84] X. Yang, A. Vorobiev, A. Generalov, M. A. Andersson, and J. Stake, "A flexible graphene terahertz detector," *Appl. Phys. Lett.*, vol. 111, no. 2, 2017, doi: 10.1063/1.4993434.

[85] I. Llatser *et al.*, "Characterization of graphene-based nano-antennas in the terahertz band," in *Proc. 6th Eur. Conf. Antennas Propag.*, 2012, pp. 194–198, doi: 10.1109/EuCAP.2012.6206598.

[86] M. K. Azizi, M. A. Ksiksi, H. Ajlani, and A. Gharsallah, "Terahertz graphene-based reconfigurable patch antenna," *Prog. Electromagn. Res. Lett.*, vol. 71, pp. 69–76, 2017, doi: 10.2528/pierl17081402.

[87] M. Letellier, J. Macutkevic, P. Kuzhir, J. Banys, V. Fierro, and A. Celzard, "Electromagnetic properties of model vitreous carbon foams," *Carbon N.Y.*, vol. 122, pp. 217–227, 2017, doi: 10.1016/j.carbon.2017.06.080.

[88] J. Song *et al.*, "Efficient excitation of multiple plasmonic modes on three-dimensional graphene: An unexplored dimension," *ACS Photon.*, vol. 3, no. 10, pp. 1986–1992, 2016, doi: 10.1021/acsphotonics.6b00566.

[89] S. Asgari, N. Granpayeh, and T. Fabritius, "Controllable terahertz cross-shaped three-dimensional graphene intrinsically chiral metastructure and its biosensing application," *Opt. Commun.*, vol. 474, 2020, Art. no. 126080, doi: 10.1016/j.optcom.2020.126080.

[90] M. Dragoman *et al.*, "Coplanar waveguide on graphene in the range 40 MHz-110 GHz," *Appl. Phys. Lett.*, vol. 99, no. 3, 2011, doi: 10.1063/1.3615289.

[91] A. Nejati, R. A. Sadeghzadeh, and F. Geran, "Effect of photonic crystal and frequency selective surface implementation on gain enhancement in the microstrip patch antenna at terahertz frequency," *Phys. B Condens. Matter*, vol. 449, pp. 113–120, 2014, doi: 10.1016/j.physb.2014.05.014.

[92] C. I. Idumah and A. Hassan, "Emerging trends in graphene carbon based polymer nanocomposites and applications," *Rev. Chem. Eng.*, vol. 32, no. 2, pp. 223–264, 2016, doi: 10.1515/revce-2015-0038.

[93] M. Zhang and J. T. W. Yeow, "Flexible polymer-carbon nanotube composite with high-response stability for wearable thermal imaging," *ACS Appl. Mater. Interfaces*, vol. 10, no. 31, pp. 26604–26609, 2018, doi: 10.1021/acsami.8b06482.